

Coherent phase slips in coupled matter-wave circuits

A. Pérez-Obiol^{1,*}, J. Polo^{2,*} and L. Amico^{3,4,5,§}¹Barcelona Supercomputing Center, 08034 Barcelona, Spain²Quantum Research Centre, Technology Innovation Institute, Abu Dhabi, United Arab Emirates³INFN-Sezione di Catania, Via Santa Sofia 64, 95127 Catania, Italy⁴Centre for Quantum Technologies, National University of Singapore, 3 Science Drive 2, Singapore 117543, Singapore⁵LANEF “Chaire d’Excellence”, Université Grenoble-Alpes & CNRS, F-38000 Grenoble, France

(Received 20 December 2021; accepted 18 March 2022; published 17 May 2022)

Quantum phase slips are a dual process of particle tunneling in coherent networks. Besides being of central interest to condensed matter physics, quantum phase slips are resources that are sought to be manipulated in quantum circuits. Here, we devise a specific matter-wave circuit enlightening quantum phase slips. Specifically, we investigate the quantum many-body dynamics of two side-by-side ring-shaped neutral bosonic systems coupled through a weak link. By imparting a suitable magnetic flux, persistent currents flow in each ring with given winding numbers. We demonstrate that coherent phase slips occur as winding number transfer among the two rings, with the populations in each ring remaining nearly constant. Such a phenomenon occurs as a result of a specific entanglement of circulating states, that, as such, cannot be captured by a mean-field treatment of the system. Our work can be relevant for the observation of quantum phase slips in cold-atom experiments and their manipulation in matter-wave circuits. To make contact with the field, we show that the phenomenon has clear signatures in the momentum distribution of the system providing the time-of-flight image of the condensate.

DOI: [10.1103/PhysRevResearch.4.L022038](https://doi.org/10.1103/PhysRevResearch.4.L022038)

Introduction. Phase slips are jumps of the phase of the wave function. In coherent systems such as superconducting and cold-atom networks, they occur because of the suppression of the amplitude of the superconducting/superfluid order parameter making the phase unrestricted and able to jump by a discrete amount (in multiples of 2π) [1,2]. When such suppression is caused by thermal fluctuations, a thermal phase slip occurs. Quantum phase slips (QPSs), instead, are induced by quantum fluctuations. A way to engineer QPSs in mesoscopic physics is through Josephson junctions, in which such events correspond to tunneling of the phase of the order parameter [1,3]. Intriguingly, relying on a phase-charge duality, it was argued that such tunneling events occur in proximity to the Coulomb-blocked regime [4,5].

In cold-atom settings, QPSs have been investigated in different settings with enhanced control and flexibility of the physical conditions [6–10]. Atomtronic circuits, in particular, define coherent networks to study mesoscopic effects and quantum transport of ultracold atoms [11–15]. In the interesting configuration of bosonic condensates in a toroidal

geometry, thermal and QPSs have been suggested as the main mechanisms responsible for the dynamics of the atoms’ persistent flow through the nucleation of vortex states and associated phonon emission, or through the formation of dark solitons activated thermally or by the stirring protocol [16–23].

Although over the past three decades several phenomena in superconducting networks have been related to QPSs’ formation [24–31], convincing experimental evidence of their occurrence in solid state physics has been obtained only recently [32]. In cold atoms, instead, QPSs, as a coherent transfer of vortices or flux, have not been observed yet.

Besides their interest in fundamental physics, QPSs can be a *resource* for quantum technology. Josephson-junction-based quantum devices harnessing QPSs have been carried out [31,33,34]. For atomtronic ring circuits interrupted by weak links, defining the atomic counterparts of SQUID devices, QPSs localized at the weak link play a crucial role for creating the superposition of the current states that is expected to be especially important for quantum sensing [21,35–39].

Relying on the considerable know-how achieved in magneto-optic circuit design and atom manipulation techniques, integrated atomtronic circuits define an interesting direction of the field [12,13]. In this context, simple circuits of coupled rings and waveguides have been considered [37,40–49]. Coupled-ring condensates, in particular, are prototype systems for the definition of coherent cold-atom networks in which matter-wave flows are manipulated as a resource. Even though several attempts have been done in this direction, the analyses carried out so far show that independent winding numbers can coexist in the two rings separately [45,46]. The transfer of winding numbers, though, has not been achieved.

*These authors contributed equally to this work.

†axel.perezobiol@bsc.es

‡juan.polo@tii.ae

§On leave from Dipartimento di Fisica e Astronomia “Ettore Majorana”, Università di Catania, Catania, Italy.

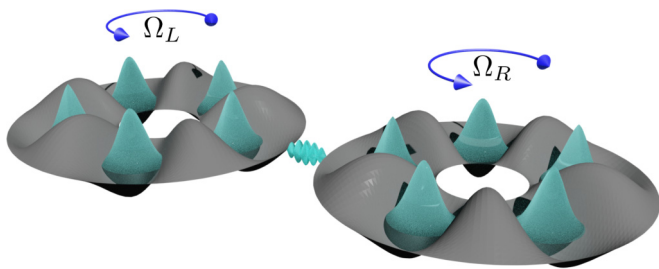


FIG. 1. Schematic diagram of an optical lattice consisting of two-sided rings of five sites each. We represent the small link between rings, t_l , with a small interfering pattern connecting the rings. Both rings have an effective artificial gauge field denoted by Ω_L and Ω_R .

Here, we solve the above bottleneck and demonstrate a coherent QPS in two coupled rings arranged side-by-side as in Fig. 1. Bosonic particles in a side-by-side geometry, with no external artificial gauge fields, has already been realized in experiment with high control on tunneling rates and on-site interactions [50]; see also [51,52]. In the two rings system devised here, matter-wave currents with different winding numbers are assumed to be imparted through effective magnetic flux [53], feasible with suitable laser fields [12,13], through phase mask or trap depth manipulation [54]. We will argue that to observe such an effect it is important that the system work in the full-fledged quantum regime. Indeed, the QPS that we observe results from an oscillation of entangled states of angular momentum states of the two rings.

The model. We consider a system of bosonic atoms trapped in a lattice of two coupled coplanar rings, each of N_s sites, and subjected to an effective magnetic flux Ω_α , $\alpha = L, R$. See Fig. 1 for a schematic picture of the system. The system's Hamiltonian reads

$$H = H_L + H_R + H_l(\tau),$$

$$H_\alpha = \sum_{i=0}^{N_s-1} \left[\frac{U}{2} (\hat{n}_{\alpha,i}^2 - \hat{n}_{\alpha,i}) - t \left(e^{-i\frac{2\pi\Omega_\alpha}{N_s}} \hat{a}_{\alpha,i}^\dagger \hat{a}_{\alpha,i+1} + \text{H.c.} \right) \right],$$

$$H_l(\tau) = -t_l(\tau) (\hat{a}_{L,0}^\dagger \hat{a}_{R,0} + \hat{a}_{R,0}^\dagger \hat{a}_{L,0}). \quad (1)$$

$\hat{a}_{\alpha,i}$ and $\hat{a}_{\alpha,i}^\dagger$ annihilate and create, respectively, a boson in the site i of the ring α , satisfying periodic conditions $\hat{a}_{\alpha,N_s} = \hat{a}_{\alpha,0}$, $\hat{a}_{\alpha,N_s}^\dagger = \hat{a}_{\alpha,0}^\dagger$, and the bosonic number operator is $\hat{n}_{\alpha,i} = \hat{a}_{\alpha,i}^\dagger \hat{a}_{\alpha,i}$. The parameters t and $U \geq 0$ are the intra-ring hopping amplitude and repulsive interaction; t_l describes the tunneling among the two rings. We set $t = 1$.

The limits $U = 0$ and $U \rightarrow \infty$ can be treated analytically for $t_l = 0$. The former reduces to the one-particle problem, while the latter maps to tight-binding hard-core bosons [55]. We focus on the regime with weak inter-ring coupling $t_l < t$, allowing us to work out both the numerical simulations obtained by exact diagonalization and perturbative analysis in t_l/t .

For uncoupled symmetric rings, $t_l = \Omega_L = \Omega_R = 0$, the energy spectrum is invariant under the exchange of left and right states, or under the inversion of angular momentum directions in each separate ring, resulting in specific degeneracies in the spectrum of (1).

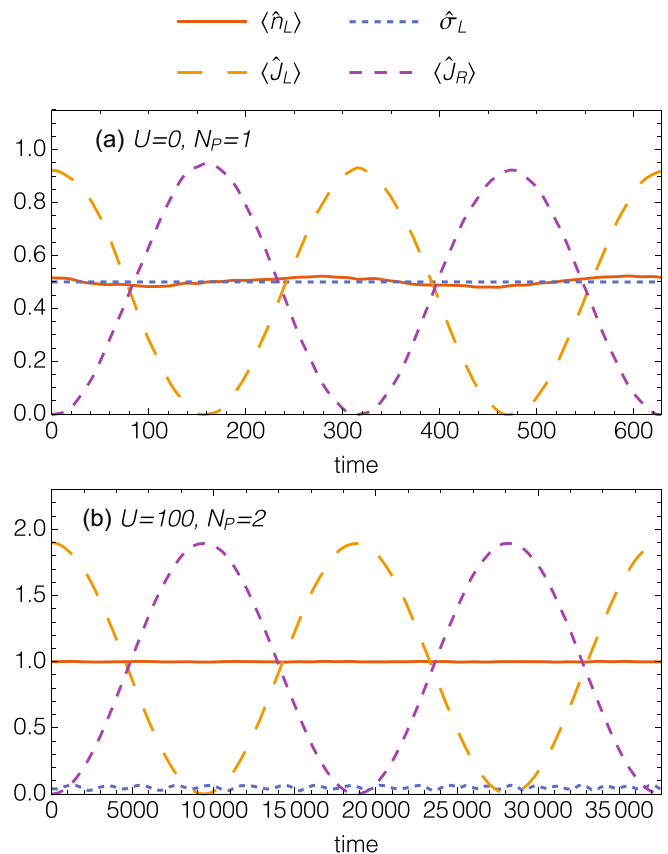


FIG. 2. Particle number's expectation value, standard deviation, and current oscillations after quenching a system of two rings of five sites, $N_s = 5$, and $t_l = 0.05$. The initial fluxes are $\Omega_L = 1$, $\Omega_R = 0$ and the final ones $\Omega_L = \Omega_R = 0.05$. (a) Noninteracting (single-particle) case, $U = 0$, $N_p = 1$. (b) Interactions set to $U = 100$ and $N_p = 2$ ($N_p > 2$ is considered in Fig. 4). See Fig. 3 to compare the periods for different t_l .

For $\Omega_L = \Omega_R > 0$, the rotational symmetry is broken, and clockwise and counterclockwise current states split into separate energy levels. In this regime, the eigenstates are found to be either nondegenerate or twofold degenerate. A finite t_l splits the remaining degenerate energy levels, and the new eigenvectors become a superposition of the uncoupled degenerate states. We shall see that such level splitting is important for the formation of specific entangled states enabling the QPS (see Supplemental Material [56] for an example of such energy splittings).

Quench protocol. We first construct a state with the same density of particles in each ring, $\frac{N_p}{2}$, but with zero angular momentum on the right, $\langle J_R \rangle = 0$, and a nonvanishing current on the left, $\langle J_L \rangle \doteq J_{\max}$. We denote such state as $|L_j; R_0\rangle \doteq |\frac{N_p}{2}, J_{\max}; \frac{N_p}{2}, 0\rangle$, resulting to be an eigenstate of the system when $\Omega_L = j$, $\Omega_R = 0$, with j integer. Next, we perform the quench on the system to $\Omega_L = \Omega_R \gtrsim 0$. Then, the state $|L_j; R_0\rangle$ is a superposition of quasidegenerate eigenvectors, each with the same particle number $\frac{N_p}{2}$ and total current J_{\max} . After the quench, a time evolution occurs on the expectation

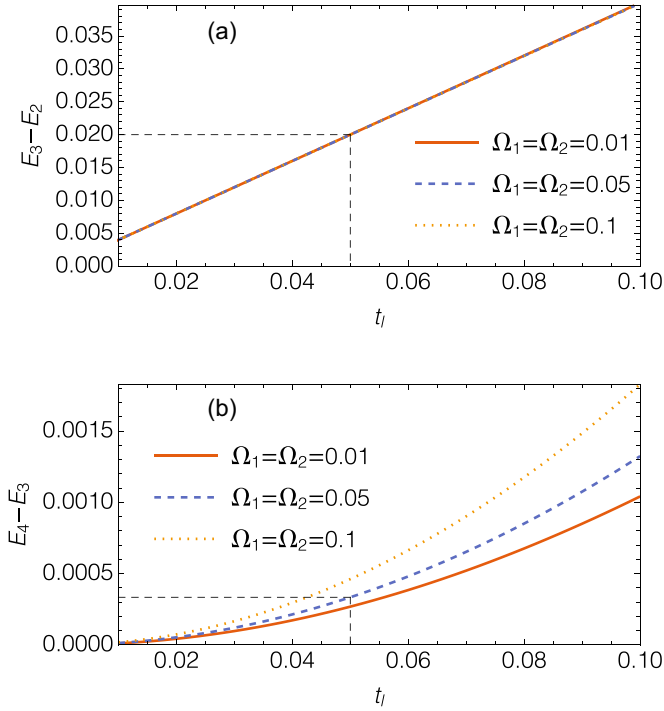


FIG. 3. Energy gap (such that periods $T = \frac{2\pi}{\Delta E}$) as a function of the interring coupling t_l and $\Omega_L = \Omega_R = 0.01, 0.05, 0.1$ for (a) one particle ($\Delta E = \frac{2t_l}{N_s}$), (b) two particles and $U = 100$ ($\Delta E \propto t_l^2$). Dashed black lines in both plots mark the energy gaps for $t_l = 0.05$, corresponding to $T = 314$ (a) and $T = 18793$ (b), the periods in Fig. 2.

value of the number of particles $\langle \hat{n}_\alpha \rangle$, its variance σ_α^2 , and the current $\langle J_\alpha \rangle$, defined as

$$\sigma_\alpha^2 = \langle \hat{n}_\alpha^2 \rangle - \langle \hat{n}_\alpha \rangle^2, \quad (2)$$

$$\langle J_\alpha \rangle = -i \sum_k \langle \hat{a}_{\alpha,k}^\dagger \hat{a}_{\alpha,k+1} - \hat{a}_{\alpha,k+1}^\dagger \hat{a}_{\alpha,k} \rangle, \quad (3)$$

with $\hat{n}_\alpha = \sum_i \hat{n}_{\alpha,i}$.

Results. Current oscillations between left and right rings are found for small and large interactions, $U \lesssim 0.01$ and $U \gtrsim 10$, when following the quench. See Fig. 2 for the cases $U = 0$ and $U = 100$. The currents in each ring oscillate completely out of phase, between a maximum value J_{\max} and zero:

$$|L(\tau); R(\tau)\rangle = \cos(\omega \tau) |L_j; R_0\rangle + \sin(\omega \tau) |L_0; R_j\rangle, \quad (4)$$

with $\omega = \frac{\Delta E}{2\pi}$, ΔE being the energy gap between the involved states. Importantly, the expectation number $\langle \hat{n}_\alpha \rangle$ in each of the two rings results in being nearly constant at all times: no net transfer of particles between rings occurs and current oscillations happen due to the phase slipping through the weak link. Note that the phase by itself does not carry any angular momentum or direction, and for the current to change, an arbitrary small flux $\Omega_{L/R} = \Omega_\alpha$ is required to be applied in each ring.

The specific particle configuration n_α and σ_α^2 , and the maximum current J_{\max} in $|L_j; R_0\rangle$ and $|L_0; R_j\rangle$ depend on U and N_p (see Table I and Supplemental Material [56] for a more detailed analysis). By using perturbation analysis, we find

TABLE I. Expected value of the occupation and variance in each ring, amplitude and period ($T = 2\pi/\omega$) of current oscillations, in the case of no interactions and for $U \rightarrow \infty$.

	$\langle \hat{n} \rangle \sigma^2$	J_{\max}	Period
$U = 0$	$\frac{N_p}{2} \frac{N_p}{4}$	$N_p \sin\left(\frac{2\pi}{N_s}\right)$	$\frac{\pi N_s}{t_l}$
$U \rightarrow \infty$ N_p even	$\frac{N_p}{2} \ 0$	$4(N_b + 1) \cos\left(\frac{\pi}{N_s}\right) \sin\left(\frac{\pi N_e}{2N_s}\right)$	$\propto \frac{1}{t_l^2}$
N_p odd	$\frac{N_p}{2} \ \frac{1}{4}$	$4(N_b + 1) \cos\left(\frac{\pi}{N_s}\right) \cos\left(\frac{\pi}{2N_s}\right) \sin\left(\frac{\pi N_e}{2N_s}\right)$	$\propto \frac{1}{t_l}$

that ω depends linearly on t_l for $U = 0$, and quadratically for large U (except for odd N_p ; see Fig. 3 and Table I). Important insights on the effect of the interaction can be obtained by studying the limit $U \rightarrow \infty$ (see Supplemental Material [56] for more details on the U and t_l dependence). Although the expected number of particles results in being barely affected by U , its variance σ_α does. For $U = 0$, $\sigma_\alpha^2 = \frac{N_p}{4}$. For large interactions, instead, any measurement of the occupation would always find half the particles in each ring, and therefore $\sigma_\alpha^2 = 0$ is found (or $\frac{N_p \pm 1}{2}$ particles in each ring and $\sigma_\alpha^2 = \frac{1}{4}$ for N_p odd). We also remark that, because of the particle-hole symmetry holding for large interactions, QPSs for holes occur similarly to the particle ones (see Fig. 4). As for the maximum current, in the case of $U = 0$, it results in scaling linearly with the number of particles, $J_{\max} = N_p \sin\left(\frac{2\pi}{N_s}\right)$, while for large interactions we find $J_{\max} \propto (N_b + 1) \sin\left(\frac{2\pi N_e}{2N_s}\right)$, with N_b and N_e the background and excess of particles such that $N_p = 2N_s \times N_b + N_e$. To transfer larger currents, one can simply start with an integer flux Ω_L in $1 < n < k_{\max}$. Numerical tests

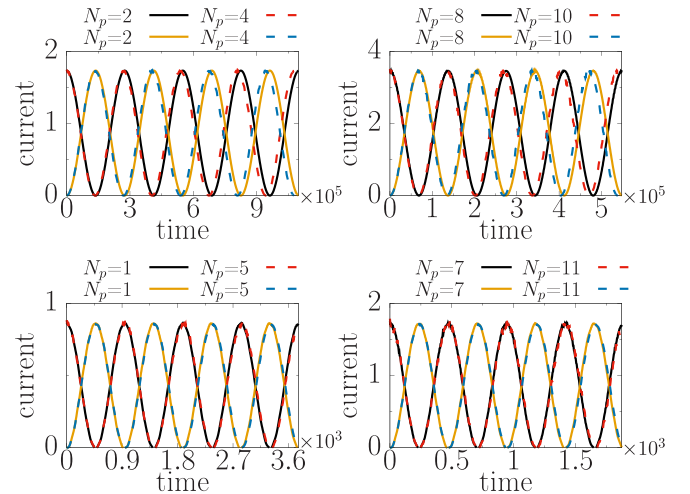


FIG. 4. Each plot compares QPSs where (excess) particles N_e and holes $2N_s - N_e$ are exchanged in the strongly interacting regime, $U = 1000$, and in rings of $N_s = 3$ sites. Particle-hole symmetry is displayed for two different commensurate fillings, such that the total number of particles is $N_p = 2N_s \times N_b + N_e$, with $N_b = 0$ (left plots) and $N_b = 1$ (right plots), and $N_e = \{2, 4\}$ (top plots) and $N_e = \{1, 5\}$ (bottom plots). We quench from $\Omega_L = 1, \Omega_R = 0$, to $\Omega_L = 0.01, \Omega_R = 0.01$, and from $t_l = 10^{-5}$ to $t_l = 0.01$. Note that the period substantially changes for each commensurate filling $N_b = 0, 1$, despite having the same number of particles and holes. These changes appear because the energy levels shift proportionally to N_b .

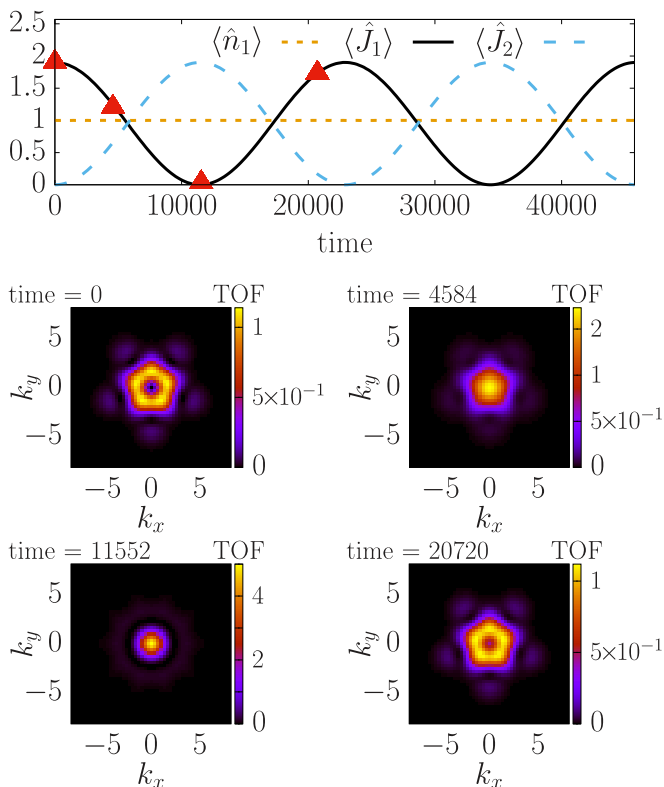


FIG. 5. Time-of-flight expansion of the left ring. Parameters are $\Omega_L = 1$, $\Omega_R = 0$ to $\Omega_L = 0.01$, $\Omega_R = 0.01$, $t_i = 0$ to $t_f = 0.05$, $N_p = 2$, $N_s = 5$ in each ring, $U = 10$. Triangles indicate the times at which the TOF snapshots were taken.

for various ring sizes and initial currents corroborate that QPSs are still found as N_p and angular momenta are increased (see Fig. 4).

By controlling t_i in time, and relying on our condition of weak ring-ring coupling, we note that different entangled states of angular momenta can be engineered by our scheme. The transfer of angular momentum can be obtained by manipulating t_i on $\tau = \frac{T}{2} \times (2n + 1)$, with T the period. For $\tau = \frac{T}{4} \times (2n + 1)$, for example, the entangled state $|L_j; R_0\rangle + |L_0; R_j\rangle$ can be achieved.

Readout of the QPSs. Matter-wave currents can be detected through time-of-flight (TOF) measurements [57,58]. Such measurements in the far field are directly related to the momentum distribution at the moment in which the condensate is released from the ring trap. Therefore, the time evolution of the persistent current is reflected in the time evolution of the momentum distribution: $n(\mathbf{k}, \tau) = \sum_{i,j} e^{i\mathbf{k} \cdot (\mathbf{R}_i - \mathbf{R}_j)} C_{i,j}(\tau)$ with $C_{i,j}(\tau) = \langle \psi(\tau) | a_i^\dagger a_j | \psi(\tau) \rangle$ being the one-body correlation function between different sites and \mathbf{R}_j denoting the position of the lattice sites of the ring. In each ring, we find that $n(\mathbf{k}, \tau)$ evolves from a peak momentum distribution to the characteristic circular-shaped one as soon as the system acquires one unit of angular momentum. Such dynamics in the TOF provides the readout of the transfer of coherent phase slips between zero and one unit of angular momentum. See Fig. 5.

Discussion and conclusions. We have theoretically demonstrated QPSs between two tunnel-coupled rings of interacting

bosons: We prepare two different phase states of the two separated rings; after quenching the tunnel between the rings, we observe a coherent oscillation between the phase states with nearly vanishing population fluctuations (in each of the two rings). Once calibrated, the scheme can be used to produce, transfer, and entangle current states by turning on and off the weak link at specific times after the quenching protocol. We find that the phase slips faster from one ring to the other for stronger inter-ring couplings. Interactions reduce the maximum current in each ring, and make phase slips slower (see Supplemental Material [56] for the interplay between interactions and period of oscillations). Indeed, such phenomenon occurs as a direct consequence of the entangled state created between the phase states of the two rings (macroscopic superposition of all particles rotating with different angular momenta in each ring). The coherent oscillations of the QPSs are characterized by the simultaneous creation and destruction of current states in each ring (see Supplemental Material [56] for specific examples). As such, QPS transfer is a genuine quantum effect that cannot be captured by standard mean-field analysis such as a Gross-Pitaevskii based approach. In fact, the latter neglects entanglement and, to the best of our knowledge, cannot describe coherent transfer of matter-waves without transfer of population (which is an essential trait of our demonstration). We note that the coupling between the rings is perturbative and as such, the corresponding emergence of quasidegenerate states involving a superposition of left and right current states holds for large particle numbers. The scope of our results can be further enlarged by resorting to a suitable particle-hole symmetry. Therefore, our QPSs are expected to occur also in systems with large particle numbers. We studied the momentum distribution that is the standard method to analyze neutral matter-wave currents in cold-atom experiments [57–62].

Our work provides a specific platform to observe QPSs in cold atoms, which are a well known open problem in the field and a fundamental pillar in the development of quantum technologies. At the same time, our work results are relevant to progress in the implementation of integrated atomtronic circuits [12,13]. Specifically, our results effectively enable atomtronic circuits based on coupled atomic rings: In a sense analogous to the “rapid single flux quantum logic” conceived with SQUIDs [63], complex structures where the information is encoded in the phase slips inherent to the different rings could be implemented.

Our proposal is within the current know-how in ultracold-atom experiments. Coupled ring circuits have been previously investigated [50]. We note the recent advances on the design of matter wave circuits of ultracold atoms of any shape and intensity with full control and flexibility of the physical conditions as well as with multiple examples of experimentally controlling persistent currents in ring-shaped circuits (see [12,13] for a summary of the relevant experimental achievements in the field). Specifically for our scheme, relying on the microsecond refresh rates of digital micrometer devices [64,65] and the painting technique [66], it is feasible to impart the effective magnetic flux on the two different rings separately. A possible protocol could be to impart the rotation to two distant rings and then adiabatically approaching them or using phase masks, whose micrometer resolution has been demonstrated, to address each ring [67].

We thank G. Catelani and W. Jordan Chetcuti for discussion. A.P.-O. acknowledges financial support from Secretaria d'Universitats i Recerca del Departament d'Empresa i Coneixement de la Generalitat de

Catalunya cofunded by the European Union Regional Development Fund within the ERDF Operational Program of Catalunya (project QuantumCat, Ref. No. 001-P-001644).

-
- [1] K. Arutyunov, D. Golubev, and A. Zaikin, Superconductivity in one dimension, *Phys. Rep.* **464**, 1 (2008).
- [2] C. D'Errico, S. S. Abbate, and G. Modugno, Quantum phase slips: From condensed matter to ultracold quantum gases, *Philos. Trans. R. Soc. A* **375**, 20160425 (2017).
- [3] G. Rastelli, I. M. Pop, and F. W. J. Hekking, Quantum phase slips in Josephson junction rings, *Phys. Rev. B* **87**, 174513 (2013).
- [4] J. Mooij and Y. V. Nazarov, Superconducting nanowires as quantum phase-slip junctions, *Nat. Phys.* **2**, 169 (2006).
- [5] A. M. Hriscu and Y. V. Nazarov, Coulomb blockade due to quantum phase slips illustrated with devices, *Phys. Rev. B* **83**, 174511 (2011).
- [6] A. Polkovnikov, S. Sachdev, and S. M. Girvin, Nonequilibrium Gross-Pitaevskii dynamics of boson lattice models, *Phys. Rev. A* **66**, 053607 (2002).
- [7] A. Polkovnikov, E. Altman, E. Demler, B. Halperin, and M. D. Lukin, Decay of superfluid currents in a moving system of strongly interacting bosons, *Phys. Rev. A* **71**, 063613 (2005).
- [8] S. Khlebnikov and L. P. Pryadko, Quantum Phase Slips in the Presence of Finite-Range Disorder, *Phys. Rev. Lett.* **95**, 107007 (2005).
- [9] I. Danshita, Universal Damping Behavior of Dipole Oscillations of One-Dimensional Ultracold Gases Induced by Quantum Phase Slips, *Phys. Rev. Lett.* **111**, 025303 (2013).
- [10] T. Roscilde, M. F. Faulkner, S. T. Bramwell, and P. C. W. Holdsworth, From quantum to thermal topological-sector fluctuations of strongly interacting bosons in a ring lattice, *New J. Phys.* **18**, 075003 (2016).
- [11] L. Amico, G. Birkel, M. Boshier, and L.-C. Kwek, Focus on atomtronics-enabled quantum technologies, *New J. Phys.* **19**, 020201 (2017).
- [12] L. Amico *et al.*, Roadmap on atomtronics: State of the art and perspective, *AVS Quantum Sci.* **3**, 039201 (2021).
- [13] L. Amico, D. Anderson, M. Boshier, J.-P. Brantut, L.-C. Kwek, A. Minguzzi, and W. von Klitzing, Atomtronic circuits: From basic research in many-body physics to applications for quantum technologies, *arXiv:2107.08561*.
- [14] J.-P. Brantut, J. Meineke, D. Stadler, S. Krinner, and T. Esslinger, Conduction of ultracold fermions through a mesoscopic channel, *Science* **337**, 1069 (2012).
- [15] A. Burchianti, F. Scazza, A. Amico, G. Valtolina, J. A. Seman, C. Fort, M. Zaccanti, M. Inguscio, and G. Roati, Connecting Dissipation and Phase Slips in a Josephson Junction between Fermionic Superfluids, *Phys. Rev. Lett.* **120**, 025302 (2018).
- [16] K. C. Wright, R. B. Blakestad, C. J. Lobb, W. D. Phillips, and G. K. Campbell, Driving Phase Slips in a Superfluid Atom Circuit with a Rotating Weak Link, *Phys. Rev. Lett.* **110**, 025302 (2013).
- [17] A. Ramanathan, K. C. Wright, S. R. Muniz, M. Zelan, W. T. Hill, C. J. Lobb, K. Helmerson, W. D. Phillips, and G. K. Campbell, Superflow in a Toroidal Bose-Einstein Condensate: An Atom Circuit with a Tunable Weak Link, *Phys. Rev. Lett.* **106**, 130401 (2011).
- [18] S. Eckel, J. G. Lee, F. Jendrzejewski, N. Murray, C. W. Clark, C. J. Lobb, W. D. Phillips, M. Edwards, and G. K. Campbell, Hysteresis in a quantized superfluid "atomtronic" circuit, *Nature (London)* **506**, 200 (2014).
- [19] A. I. Yakimenko, Y. M. Bidasnyuk, M. Weyrauch, Y. I. Kuriatnikov, and S. I. Vilchinskii, Vortices in a toroidal Bose-Einstein condensate with a rotating weak link, *Phys. Rev. A* **91**, 033607 (2015).
- [20] J. Polo, V. Ahufinger, F. W. J. Hekking, and A. Minguzzi, Damping of Josephson Oscillations in Strongly Correlated One-Dimensional Atomic Gases, *Phys. Rev. Lett.* **121**, 090404 (2018).
- [21] J. Polo, R. Dubessy, P. Pedri, H. Perrin, and A. Minguzzi, Oscillations and Decay of Superfluid Currents in a One-Dimensional Bose Gas on a Ring, *Phys. Rev. Lett.* **123**, 195301 (2019).
- [22] A. Pérez-Obiol and T. Cheon, Bose-Einstein condensate confined in a one-dimensional ring stirred with a rotating delta link, *Phys. Rev. E* **101**, 022212 (2020).
- [23] A. Pérez-Obiol, J. Polo, and T. Cheon, Current production in ring condensates with a weak link, *Phys. Rev. A* **102**, 063302 (2020).
- [24] C. N. Lau, N. Markovic, M. Bockrath, A. Bezryadin, and M. Tinkham, Quantum Phase Slips in Superconducting Nanowires, *Phys. Rev. Lett.* **87**, 217003 (2001).
- [25] A. Bezryadin, C. Lau, and M. Tinkham, Quantum suppression of superconductivity in ultrathin nanowires, *Nature (London)* **404**, 971 (2000).
- [26] A. T. Bollinger, R. C. Dinsmore, A. Rogachev, and A. Bezryadin, Determination of the Superconductor-Insulator Phase Diagram for One-Dimensional Wires, *Phys. Rev. Lett.* **101**, 227003 (2008).
- [27] F. Altomare, A. M. Chang, M. R. Melloch, Y. Hong, and C. W. Tu, Evidence for Macroscopic Quantum Tunneling of Phase Slips in Long One-Dimensional Superconducting Al Wires, *Phys. Rev. Lett.* **97**, 017001 (2006).
- [28] N. A. Masluk, I. M. Pop, A. Kamal, Z. K. Mineev, and M. H. Devoret, Microwave Characterization of Josephson Junction Arrays: Implementing a Low Loss Superinductance, *Phys. Rev. Lett.* **109**, 137002 (2012).
- [29] V. E. Manucharyan, J. Koch, L. I. Glazman, and M. H. Devoret, Fluxonium: Single cooper-pair circuit free of charge offsets, *Science* **326**, 113 (2009).
- [30] T. Weißl, B. Küng, E. Dumur, A. K. Feofanov, I. Matei, C. Naud, O. Buisson, F. W. J. Hekking, and W. Guichard, Kerr coefficients of plasma resonances in Josephson junction chains, *Phys. Rev. B* **92**, 104508 (2015).
- [31] I. M. Pop, I. Protopopov, F. Lecocq, Z. Peng, B. Pannetier, O. Buisson, and W. Guichard, Measurement of the effect of quantum phase slips in a Josephson junction chain, *Nat. Phys.* **6**, 589 (2010).
- [32] O. Astafiev, L. Ioffe, S. Kafanov, Y. A. Pashkin, K. Y. Arutyunov, D. Shahar, O. Cohen, and J. S. Tsai, Coherent quantum phase slip, *Nature (London)* **484**, 355 (2012).

- [33] J. E. Mooij and C. J. P. M. Harmans, Phase-slip flux qubits, *New J. Phys.* **7**, 219 (2005).
- [34] A. Belkin, M. Belkin, V. Vakaryuk, S. Khlebnikov, and A. Bezryadin, Formation of Quantum Phase Slip Pairs in Superconducting Nanowires, *Phys. Rev. X* **5**, 021023 (2015).
- [35] M. Cominotti, D. Rossini, M. Rizzi, F. Hekking, and A. Minguzzi, Optimal Persistent Currents for Interacting Bosons on a Ring with a Gauge Field, *Phys. Rev. Lett.* **113**, 025301 (2014).
- [36] D. Aghamalyan, N. T. Nguyen, F. Auksztol, K. S. Gan, M. M. Valado, P. C. Condylis, L.-C. Kwek, R. Dumke, and L. Amico, An atomtronic flux qubit: A ring lattice of Bose-Einstein condensates interrupted by three weak links, *New J. Phys.* **18**, 075013 (2016).
- [37] L. Amico, D. Aghamalyan, F. Auksztol, H. Crepaz, R. Dumke, and L. C. Kwek, Superfluid qubit systems with ring shaped optical lattices, *Sci. Rep.* **4**, 4298 (2015).
- [38] C. Ryu, P. W. Blackburn, A. A. Blinova, and M. G. Boshier, Experimental Realization of Josephson Junctions for an Atom SQUID, *Phys. Rev. Lett.* **111**, 205301 (2013).
- [39] J. Polo, P. Naldesi, A. Minguzzi, and L. Amico, The quantum solitons atomtronic interference device, *Quantum Sci. Technol.* **7**, 015015 (2022).
- [40] S. Safaei, L.-C. Kwek, R. Dumke, and L. Amico, Monitoring currents in cold-atom circuits, *Phys. Rev. A* **100**, 013621 (2019).
- [41] A. Escrivà, A. Richaud, B. Juliá-Díaz, and M. Guilleumas, Static properties of two linearly coupled discrete circuits, *J. Phys. B: At., Mol. Opt. Phys.* **54**, 115301 (2021).
- [42] A. Richaud and V. Penna, Quantum dynamics of bosons in a two-ring ladder: Dynamical algebra, vortexlike excitations, and currents, *Phys. Rev. A* **96**, 013620 (2017).
- [43] D. Aghamalyan, L. Amico, and L. C. Kwek, Effective dynamics of cold atoms flowing in two ring-shaped optical potentials with tunable tunneling, *Phys. Rev. A* **88**, 063627 (2013).
- [44] J. Polo, J. Mompert, and V. Ahufinger, Geometrically induced complex tunnelings for ultracold atoms carrying orbital angular momentum, *Phys. Rev. A* **93**, 033613 (2016).
- [45] G. Pelegrí, A. M. Marques, V. Ahufinger, J. Mompert, and R. G. Dias, Second-order topological corner states with ultracold atoms carrying orbital angular momentum in optical lattices, *Phys. Rev. B* **100**, 205109 (2019).
- [46] T. Bland, Q. Marolleau, P. Comaron, B. Malomed, and N. Proukakis, Persistent current formation in double-ring geometries, *J. Phys. B: At., Mol. Opt. Phys.* **53**, 115301 (2020).
- [47] A. Gallemí, A. Muñoz Mateo, R. Mayol, and M. Guilleumas, Coherent quantum phase slip in two-component bosonic atomtronic circuits, *New J. Phys.* **18**, 015003 (2016).
- [48] A. Escrivà, A. M. Mateo, M. Guilleumas, and B. Juliá-Díaz, Tunneling vortex dynamics in linearly coupled Bose-Hubbard rings, *Phys. Rev. A* **100**, 063621 (2019).
- [49] E. Nicolau, J. Mompert, B. Juliá-Díaz, and V. Ahufinger, Orbital angular momentum dynamics of Bose-Einstein condensates trapped in two stacked rings, *Phys. Rev. A* **102**, 023331 (2020).
- [50] M. R. Sturm, M. Schlosser, R. Walser, and G. Birkl, Quantum simulators by design: Many-body physics in reconfigurable arrays of tunnel-coupled traps, *Phys. Rev. A* **95**, 063625 (2017).
- [51] T. A. Bell, J. A. P. Glidden, L. Humbert, M. W. J. Bromley, S. A. Haine, M. J. Davis, T. W. Neely, M. A. Baker, and H. Rubinsztein-Dunlop, Bose-Einstein condensation in large time-averaged optical ring potentials, *New J. Phys.* **18**, 035003 (2016).
- [52] G. Gauthier, T. A. Bell, A. B. Stilgoe, M. Baker, H. Rubinsztein-Dunlop, and T. W. Neely, *Dynamic high-resolution optical trapping of ultracold atoms*, in Advances in Atomic, Molecular, and Optical Physics (Academic Press, 2021), pp. 1–101.
- [53] J. Dalibard, F. Gerbier, G. Juzeliunas, and P. Öhberg, Colloquium: Artificial gauge potentials for neutral atoms, *Rev. Mod. Phys.* **83**, 1523 (2011).
- [54] T. Haug, R. Dumke, L.-C. Kwek, C. Miniatura, and L. Amico, Machine-learning engineering of quantum currents, *Phys. Rev. Research* **3**, 013034 (2021).
- [55] Y. Wu and X. Yang, Bose-Hubbard model on a ring: Analytical results in a strong interaction limit and incommensurate filling, *J. Opt. Soc. Am. B* **23**, 1888 (2006).
- [56] See Supplemental Material at <http://link.aps.org/supplemental/10.1103/PhysRevResearch.4.L022038> for a more detailed analysis.
- [57] S. Moulder, S. Beattie, R. P. Smith, N. Tammuz, and Z. Hadzibabic, Quantized supercurrent decay in an annular Bose-Einstein condensate, *Phys. Rev. A* **86**, 013629 (2012).
- [58] L. Amico, A. Osterloh, and F. Cataliotti, Quantum Many Particle Systems in Ring-Shaped Optical Lattices, *Phys. Rev. Lett.* **95**, 063201 (2005).
- [59] M. Greiner, O. Mandel, T. Esslinger, T. W. Hänsch, and I. Bloch, Quantum phase transition from a superfluid to a Mott insulator in a gas of ultracold atoms, *Nature (London)* **415**, 39 (2002).
- [60] F. Gerbier, A. Widera, S. Fölling, O. Mandel, T. Gericke, and I. Bloch, Interference pattern and visibility of a Mott insulator, *Phys. Rev. A* **72**, 053606 (2005).
- [61] Y. Kato, Q. Zhou, N. Kawashima, and N. Trivedi, Sharp peaks in the momentum distribution of bosons in optical lattices in the normal state, *Nat. Phys.* **4**, 617 (2008).
- [62] A. Hoffmann and A. Pelster, Visibility of cold atomic gases in optical lattices for finite temperatures, *Phys. Rev. A* **79**, 053623 (2009).
- [63] K. K. Likharev and V. K. Semenov, RSFQ logic/memory family: A new Josephson-junction technology for sub-terahertz-clock-frequency digital systems, *IEEE Trans. Appl. Supercond.* **1**, 3 (1991).
- [64] H. Rubinsztein-Dunlop, A. Forbes, M. V. Berry, M. R. Dennis, D. L. Andrews, M. Mansuripur, C. Denz, C. Alpmann, P. Banzer, T. Bauer *et al.*, Roadmap on structured light, *J. Opt.* **19**, 013001 (2017).
- [65] G. Gauthier, I. Lenton, N. M. Parry, M. Baker, M. J. Davis, H. Rubinsztein-Dunlop, and T. W. Neely, Direct imaging of a digital-micromirror device for configurable microscopic optical potentials, *Optica* **3**, 1136 (2016).
- [66] K. Henderson, C. Ryu, C. MacCormick, and M. G. Boshier, Experimental demonstration of painting arbitrary and dynamic potentials for Bose-Einstein condensates, *New J. Phys.* **11**, 043030 (2009).
- [67] A. Kumar, R. Dubessy, T. Badr, C. De Rossi, M. de Goër de Herve, L. Longchambon, and H. Perrin, Producing superfluid circulation states using phase imprinting, *Phys. Rev. A* **97**, 043615 (2018).